International Journal of Research and Review
[Indexed, Peer-Reviewed Journal]
Volume 13; Issue: 6; June 2026
Website: www.ijrrjournal.com
Research Paper *E-ISSN: 2349-9788; P-ISSN: 2454-2237*

Computational Evaluation of CeO_2-Modified Tungsten Borate Glasses as Lead-Free Gamma-Ray Shielding Materials

Oki Ade Putra[1], Zaenul Muhlisin[1], Much. Azam[1], Pandji Triadyaksa[1]

[1]Department of Physics, Faculty of Science and Mathematic, Universitas Diponegoro, Semarang, Indonesia

Corresponding Author: Oki Ade Putra

DOI: https://doi.org/10.52403/ijrr.20260616

ABSTRACT

Lead-free glasses are continuously developed as safer and more flexible alternatives to conventional radiation shielding materials such as lead and concrete. This study computationally evaluated four CeO_2-modified tungsten borate glass samples with the base composition $xCeO_2$–$(55–x)B_2O_3$–$35WO_3$–5MgO–5CaO (x = 0, 5, 10, 15 mol%), labeled CeB1–CeB4. The glass density increased almost linearly from 4.39 $g·cm^{-3}$ (CeB1) to 4.50 $g·cm^{-3}$ (CeB4) with increasing CeO_2 fraction. Radiation shielding parameters, including the mass attenuation coefficient (MAC), linear attenuation coefficient (LAC), half value layer (HVL), tenth value layer (TVL), and mean free path (MFP), were calculated using the XCOM program in the photon energy range of 0.001–15 MeV. CeB4 exhibited the highest shielding performance, particularly at low photon energies, with a markedly higher MAC than CeB1. At intermediate energy (0.5 MeV), CeB4 maintained its superiority by providing the lowest HVL, TVL, and MFP among all samples. These results indicate that CeO_2 addition enhances both density and attenuation efficiency, enabling the design of thinner and more effective glass shields. Therefore, CeO_2-modified tungsten borate glasses, especially CeB4, can be considered promising environmentally friendly candidates for lead-free radiation shielding applications.

Keywords: CeO_2; WO_3; tungsten borate glass; Lead-free glass materials; Gamma-ray shielding

INTRODUCTION

The use of ionizing radiation, such as X-rays and gamma rays, continues to increase in medical, industrial, and nuclear facility applications (1,2). However, excessive exposure to radiation can lead to long-term health effects. Therefore, effective, reliable, and environmentally friendly radiation shielding materials are required. For several decades, lead and concrete have been the primary choices. Nevertheless, the toxic nature of Pb, its very high density, and its limitations in terms of formability and optical transparency have motivated the search for alternative materials that are lighter, transparent, and lead-free (3,4).

Oxide-based glasses are emerging as promising candidates for radiation shielding applications because they can be easily fabricated, are transparent to visible light, and allow compositional engineering to control density and the content of high-Z elements. The addition of heavy metal oxides (HMOs) such as Bi_2O_3, PbO, BaO, and WO_3 has been shown to increase the mass attenuation coefficient (MAC) and the

half value layer (HVL), tenth value layer (TVL), and mean free path (MFP), making the shielding performance of glasses comparable to or even superior to that of conventional materials at certain energies (5–7). In this context, borate glass (B_2O_3) is widely used as a network former because of its low melting point, good glass-forming ability, and compatibility with various heavy metal and alkaline earth oxides (8).

WO_3 is one of the most attractive HMOs in glass-shield design because it has a high atomic number (Z = 74), high density, and a large photoelectric cross section at low to intermediate photon energies. Previous studies have shown that incorporating WO_3 significantly enhances MAC and the linear attenuation coefficient (LAC) in the low-energy region. For example, Iliyasu et al. (2024) reported that adding 10 and 20 mol% WO_3 to tellurite glass increases the MAC by 6.66% and 12.74%, respectively, at 0.015 MeV, and reduces the HVL by 6–16% compared with the reference glass (9). However, such tellurite systems still rely on costly raw materials and face issues related to chemical stability.

CeO_2, as a rare-earth metal oxide, also has strong potential in glass shielding design. Cerium (Z = 58) can exist in dual valence states (Ce^{3+}/Ce^{4+}), which affect the glass network structure, density, and radiation absorption properties. Previous studies have shown that doping CeO_2 into borate or borosilicate glasses can increase Zeff and MAC and reduce HVL and MFP, while simultaneously improving mechanical and optical properties. Abou Hussein et al. (2025) showed that the addition of CeO_2 to lead borate glass increases the density, elastic moduli, and gamma-ray absorption capability (10).

Despite these advances, the simultaneous integration of CeO_2 and WO_3 in a single glass system has rarely been explored. Solak et al. (2024) developed glasses with the composition $45B_2O_3$–$(20-x)PbO$–$30TeO_2$–$5CeO_2$–xWO_3 and found that the combination of CeO_2 and WO_3 improves hardness and shielding parameters. However, these glasses still contain significant amounts of PbO and TeO_2, raising concerns about sustainability and toxicity (11). Another study by Sayyed et al. (2025) showed that increasing BaO content in lanthanum–borate glasses significantly enhances MAC and LAC and reduces HVL and MFP, even though the system does not utilize W or Ce (12). In addition, the very high density of these glasses may pose limitations in certain applications.

Based on these studies, combinations of HMOs such as WO_3, BaO, and PbO provide high shielding performance, while CeO_2 contributes to increased density and improved mechanical properties. Computational approaches based on XCOM have become standard methods for evaluating shielding parameters. Nevertheless, several research gaps remain. Most reported systems still depend on PbO; there has been no comprehensive exploration of borate–tungstate systems with high WO_3 fractions and systematic variation of CeO_2; and quantitative studies on the correlation between CeO_2 content, density, and shielding parameters in Pb-free systems are still limited.

To address these gaps, the present study designs and computationally evaluates a CeO_2-modified tungsten borate glass system with the composition $xCeO_2$–$(55-x)B_2O_3$–$35WO_3$–$5MgO$–$5CaO$ (x = 0, 5, 10, 15 mol%). This system is selected because it combines an easily processable borate network, a high WO_3 content as the main contributor to Z and density, and CeO_2 as a modifier that can enhance shielding performance without introducing Pb toxicity. The shielding parameters MAC, LAC, HVL, TVL, and MFP are calculated using the XCOM NIST database over the photon energy range of 0.001–15 MeV. This study aims to provide a systematic understanding of the influence of CeO_2 fraction on the shielding performance of lead-free glasses and to establish a comparative basis with other glass systems for designing a new generation of radiation

shielding materials that are lighter, safer, and more efficient.

METHODS

This study evaluated the photon shielding capability of four tungsten borate glass samples modified with CeO_2. The glass system had the base composition $xCeO_2$–$(55–x)B_2O_3$–$35WO_3$–5MgO–5CaO, with x = 0, 5, 10, and 15 mol%. Each composition was treated as a homogeneous material and was used as input for the calculation of attenuation parameters using the XCOM NIST database (13). The atomic number (Z) and atomic mass (A) of all constituent elements (B, O, Mg, Ca, Ce, and W), which were required for the subsequent calculations, are listed in Table 1.

Tabel. 1 Atomic number and atomic mass of each element in the shielding glass.

Element	Atomic Number (Z)	Atomic Mass (A)
B	5	10.810
O	8	16.000
Mg	12	24.305
Ca	20	40.078
Ce	58	140.120
W	74	183.840

Four glass samples were denoted as CeB1 to CeB4, representing increasing molar fractions of CeO_2. The chemical compositions and densities of these samples are summarized in Table 2.

Tabel 2. Chemical composition and density of the glass samples.

Sampel Code	x (mol%)	Komposisi	Densitas (g/cm3)
CeB1	0	$55B_2O_3$–$35WO_3$–5MgO–5CaO	4.390
CeB2	5	$5CeO_2$–$50B_2O_3$–$35WO_3$–5MgO–5CaO	4.425
CeB3	10	$10CeO_2$–$45B_2O_3$–$35WO_3$–5MgO–5CaO	4.460
CeB4	15	$15CeO_2$–$40B_2O_3$–$35WO_3$–5MgO–5CaO	4.496

The progressive addition of CeO_2 partially replaced B_2O_3 and increased the overall glass density. The CeB4 sample, which contained the highest CeO_2 fraction, exhibited the largest density, reflecting an increase in the average effective atomic number and mass of the glass network. The elemental mass fractions (wt.%) in each sample were calculated from the molar compositions and are given in Table 3.

Tabel 3. Mass fraction of the constituent elements in the glass.

Sampel	B	O	Mg	Ca	Ce	W
CeB1	0.096	0.361	0.009	0.016	0	0.518
CeB2	0.084	0.341	0.009	0.015	0.054	0.497
CeB3	0.074	0.321	0.009	0.014	0.104	0.478
CeB4	0.063	0.303	0.008	0.014	0.151	0.461

The MAC was calculated using the XCOM program based on the NIST database, which is widely used to determine the contributions of photoelectric absorption, Compton scattering, and pair production in multicomponent materials over the photon energy range of 0.001–20 MeV (2,13). The linear attenuation coefficient (LAC, μ) describes the rate at which the radiation intensity decreases as it propagates through a material and was obtained from the Lambert–Beer law (14):

$$I = I_0 e^{-\mu x} \quad (1)$$

where I_0 and I are the photon intensities before and after passing through the glass shield, respectively, μ is the LAC (cm^{-1}), and x is the material thickness (cm). The MAC represents the attenuation capability per unit mass, allowing a fair comparison

among materials with different densities. For multicomponent systems, the total MAC was calculated using Eq. (2) (15):

$$MAC = \frac{\mu}{\rho} = \sum_i w_i \left(\frac{\mu}{\rho}\right)_i \quad (2)$$

Where wi is the mass fraction of the i-th element and (μ/ρ)i is the MAC of that element at the same photon energy.

Several derived parameters were also evaluated to assess the shielding performance of the glasses, namely the half value layer (HVL), tenth value layer (TVL), and mean free path (MFP). HVL is the thickness of material required to reduce the incident intensity to one half of its initial value, whereas TVL is the thickness required to reduce the intensity to one tenth. Both quantities were calculated directly from the LAC using Eqs. (3) and (4) (16):

$$HVL = \frac{\ln 2}{\mu} \quad (3)$$

$$TVL = \frac{\ln 10}{\mu} \quad (4)$$

Smaller HVL and TVL values indicate that a thinner glass thickness is sufficient to achieve a given attenuation level, thus reflecting better shielding performance. The MFP was defined as the average distance traveled by a photon in the material before undergoing its first interaction with the constituent atoms and was calculated using Eq. (5) (16):

$$MFP = \frac{1}{\mu} \quad (5)$$

A shorter MFP implies a higher probability of interaction within a shorter distance, indicating that the material is more effective as a radiation shield.

RESULT AND DISCUSSION

Density is a key parameter in radiation shielding performance because it is directly related to the number of electrons per unit volume that can interact with incident gamma photons (17). In the present CeO_2-modified tungsten borate glass system, increasing the molar fraction of CeO_2 from CeB1 to CeB4 led to an almost linear increase in density, from 4.39 g/cm^3 (CeB1) to 4.49 g/cm^3 (CeB4), corresponding to an increase of about 2–3% (Figure 1). This increase arises from the replacement of B_2O_3 by CeO_2, which has a higher molar mass and atomic number. A similar trend has been reported in other HMO-based glass systems, where larger HMO fractions contribute to higher densities and improved attenuation efficiency (18).

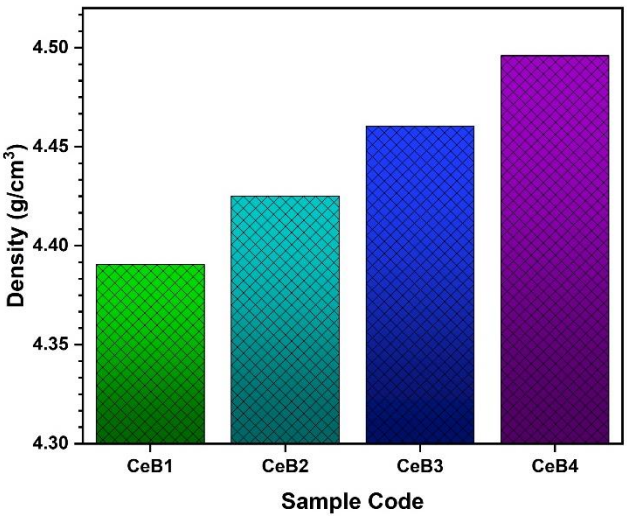

Figure 1. Density of each glass shielding sample.

The correlation between density and attenuation capability was reflected in the MAC values. At low photon energies (0.001–0.06 MeV), all samples exhibited high MAC values due to the dominance of the photoelectric effect. CeB4 consistently showed the highest MAC; for instance, at 0.06 MeV the MAC increased from 1.794 cm^2/g (CeB1) to approximately 2.968 cm^2/g (CeB4), indicating an enhancement in Zeff arising from the presence of Ce and W (10,19). As the photon energy increased, the MAC decreased sharply, indicating a transition in the dominant interaction mechanism toward the Compton region. In the intermediate energy range (0.3–1 MeV), the MAC values for all samples were on the order of 10^{-1} cm^2/g and their differences became small; at 0.5 MeV, the MAC of CeB1 and CeB4 were nearly identical (0.108 vs 0.109 cm^2/g). This behavior is consistent with the fact that Compton scattering depends primarily on the total electron density and is less sensitive to Zeff (19). The presence of the K-absorption edges of W (~0.07 MeV) and Ce (~0.04 MeV) may also give rise to local variations in the MAC curves (10,19).

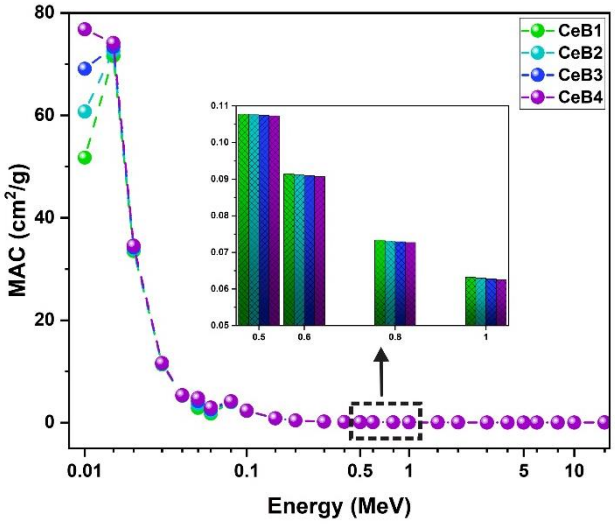

Figure 2. MAC as a function of photon energy for all samples.

The LAC values exhibited trends similar to those of MAC but expressed in units of cm^{-1}, directly representing the attenuation capacity per unit path length (Figure 3). At 0.5 MeV, the LAC of CeB4 reached 0.482 cm^{-1}, slightly higher than that of CeB1 (0.473 cm^{-1}), implying that CeB4 can provide the same level of protection with a marginally smaller thickness. Overall, the combination of a high WO_3 content and an increasing CeO_2 fraction was shown to enhance the attenuation capability, particularly at low-to-intermediate energies. At higher energies (>1 MeV), the differences between samples were not significant, suggesting that the choice of composition in this regime may be more strongly influenced by non-shielding considerations such as cost and mechanical properties. Therefore, CeO_2-modified tungsten borate glass, especially CeB4, is particularly suitable for low- and intermediate-energy radiation applications (20).

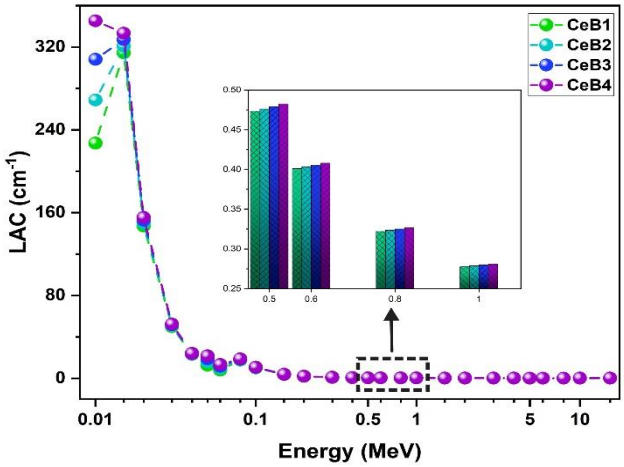

Figure 3. LAC as a function of photon energy for all samples.

The HVL, TVL, and MFP parameters provide practical insight into the material thickness required to reduce the radiation intensity. Because these quantities are inversely proportional to the LAC, their trends follow those of the LAC curves (8). At low photon energies, HVL, TVL, and MFP were small (on the order of a few millimeters), and they increased significantly at higher energies. As shown in Figure 4, the HVL of CeB1 at 0.5 MeV was 1.465 cm, whereas that of CeB4 decreased to 1.437 cm. The HVL values of CeB2 and CeB3 lay between these two limits and decreased monotonically with increasing CeO_2 fraction. This reduction in HVL from CeB1 to CeB4 indicates that the addition of CeO_2 allows a thinner glass thickness to be used to halve the incident radiation intensity (8).

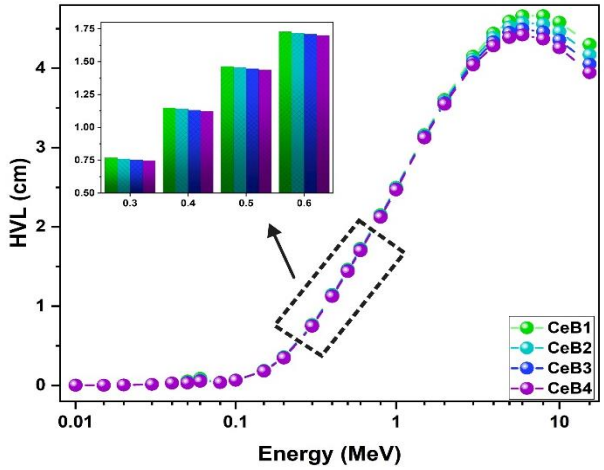

Figure 4. HVL as a function of photon energy for all samples.

The TVL values (Figure 5) followed a nearly identical trend to the HVL but were about 3.3 times higher, in accordance with their mathematical definition. At 0.5 MeV, the TVL of CeB1 was 4.865 cm, while that of CeB4 was slightly lower at 4.773 cm. This means that to reduce the radiation intensity to one tenth of its initial value, CeB4 requires a thickness that is a few millimeters thinner than CeB1. Although the absolute difference appears small, it becomes significant in large-area shielding designs, where even modest thickness reductions can decrease the total mass and structural load. These findings indicate that CeO_2 addition improves the volumetric

efficiency of the shield without compromising the intrinsic borate–tungstate glass network.

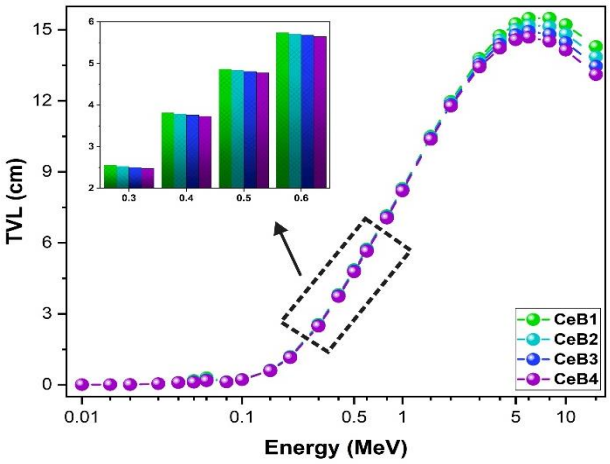

Figure 5. TVL of each glass shielding sample.

The MFP values provide another perspective on the photon interaction probability inside the glass (Figure 6). At 0.5 MeV, the MFP of CeB1 was 2.113 cm, whereas that of CeB4 decreased to 2.073 cm. In other words, photons propagating in CeB4 travel a slightly shorter average distance before undergoing their first interaction compared with those in CeB1, consistent with the higher LAC of CeB4. At low energies (≤0.1 MeV), the MFP values were on the sub-millimeter scale, indicating that photons in this energy range rapidly lose energy within relatively thin glass layers. In contrast, at energies above several MeV, the MFP increased to several centimeters and the differences among compositions diminished, reflecting the dominance of Compton scattering and pair production processes that depend more on the overall electron density than on detailed chemical composition (12). Overall, the analysis of HVL, TVL, and MFP reinforces that CeO_2 addition enhances shielding efficiency, particularly for low-to-intermediate photon energies. The CeB4 composition, with the highest CeO_2 fraction, demonstrated the best performance, making it an optimal candidate for efficient and environmentally friendly lead-free glass shields (3).

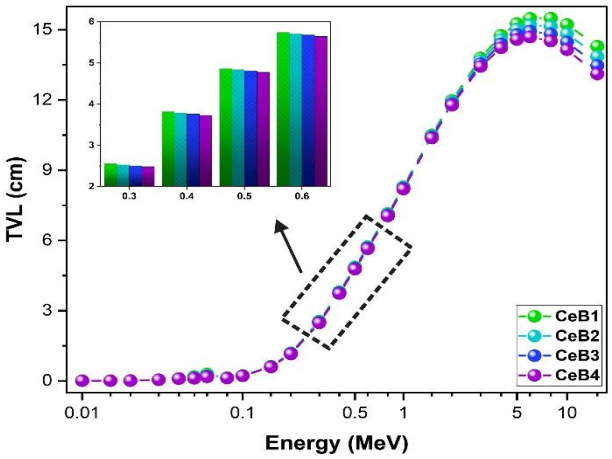

Figure 6. MFP of each glass shielding sample.

CONCLUSION

This study computationally evaluated the photon shielding performance of a lead-free glass system based on CeO_2-modified tungsten borate with the composition $xCeO_2$–$(55–x)B_2O_3$–$35WO_3$–5MgO–5CaO (x = 0, 5, 10, 15 mol%). Partial substitution of B_2O_3 by CeO_2 increases the glass density in an almost linear manner, consistent with the higher molar mass and atomic number of Ce, which contribute to an increase in Zeff. Calculations using XCOM show that at low photon energies, where the photoelectric effect dominates, the CeB4 sample exhibits the highest MAC and LAC values, indicating the most efficient radiation absorption per unit mass and per unit path length. At intermediate to high energies, the differences among compositions become narrower due to the dominance of Compton scattering, although CeB4 still maintains a moderate advantage.

The trends of the effective thickness parameters (HVL, TVL, and MFP), which are inversely related to LAC, further support these findings. CeB4 consistently shows the lowest HVL, TVL, and MFP values, particularly in the low-to-intermediate energy range that is relevant for medical and industrial applications. This behavior indicates that the required shield thickness can be reduced without compromising the protection performance.

Overall, the results demonstrate that tuning the CeO_2 fraction within a borate–tungstate matrix is an effective strategy to enhance density and attenuation efficiency without the use of PbO. Therefore, CeO_2-modified tungsten borate glasses, especially the CeB4 composition, can be considered strong candidates for a new generation of lead-free radiation shielding materials that are environmentally friendly and performance-competitive.

Declaration by Authors

Acknowledgement: None
Source of Funding: None
Conflict of Interest: The authors declare no conflict of interest.

REFERENCES

1. Abouhaswa AS, Mhareb MHA, Alalawi A, Al-Buriahi MS. Physical, structural, optical, and radiation shielding properties of B2O3-20Bi2O3- 20Na2O2- Sb2O3 glasses: Role of Sb2O3. J Non-Cryst Solids [Internet]. September 2020 [dikutip 18 Oktober 2024]; 543:120130. Tersedia pada: https://linkinghub.elsevier.com/retrieve/pii/S002230932030243X
2. Alomari AH, Al-Qahtani SM. Enhanced gamma shielding properties of borosilicate glasses with Gd2O3 addition: A theoretical study using Phy-X/PSD and XCOM programs. J Radiat Res Appl Sci [Internet]. September 2024 [dikutip 19 November 2024];17(3):100996. Tersedia pada: https://linkinghub.elsevier.com/retrieve/pii/S1687850724001808
3. Atashi P, Rahmani S, Ahadi B, Rahmati A. Efficient, flexible and lead-free composite based on room temperature vulcanizing silicone rubber/W/Bi2O3 for gamma ray shielding application. J Mater Sci Mater Electron [Internet]. Juli 2018 [dikutip 21 September 2024];29(14):12306–22. Tersedia pada: http://link.springer.com/10.1007/s10854-018-9344-1
4. Azman MN, Abualroos NJ, Yaacob KA, Zainon R. Feasibility of nanomaterial tungsten carbide as lead-free nanomaterial-based radiation shielding. Radiat Phys Chem [Internet]. Januari 2023 [dikutip 21 September 2024]; 202:110492. Tersedia pada: https://linkinghub.elsevier.com/retrieve/pii/S0969806X22005291
5. Al Huwayz M, Basha B, Alalawi A, Alrowaili ZA, Sriwunkum C, Alsaiari NS, dkk. Influence of BaO addition on gamma attenuation and radiation shielding performance of SiO2-B2O3-SrO-ZrO2 glasses. J Radiat Res Appl Sci [Internet]. Desember 2024 [dikutip 19 November 2024];17(4):101119. Tersedia pada: https://linkinghub.elsevier.com/retrieve/pii/S1687850724003030
6. Alver Ü, Duran SU, Demirköz MB, Muçogllava B, Aslan M, Çava K, dkk. Ulexite/HDPE-Bi2O3/HDPE layered composites for neutron and gamma radiation shielding. Appl Radiat Isot [Internet]. Oktober 2023 [dikutip 25 September 2024]; 200:110940. Tersedia

pada: https://linkinghub.elsevier.com/retrieve/pii/S0969804323002932

7. Biradar S, Chandrashekara MN, Dinkar A, Manjunatha, Devidas GB, Bennal AS, dkk. A multifaceted study of B2O3-BaO-PbO-WO3 glasses doped with Bi2O3: Insights from physical, thermal, structural, mechanical and optical analyses towards improved shielding properties. Ceram Int [Internet]. September 2024 [dikutip 27 Agustus 2025];50(17):29332–45. Tersedia pada: https://linkinghub.elsevier.com/retrieve/pii/S0272884224021060
8. Bengisu M. Borate glasses for scientific and industrial applications: a review. J Mater Sci [Internet]. Maret 2016 [dikutip 19 November 2024];51(5):2199–242. Tersedia pada: http://link.springer.com/10.1007/s10853-015-9537-4
9. Iliyasu U, Shehu A. Photon and Neutron Characterization of Titanium Neodymium Tellurite Glass Doped WO3. Caliphate J Sci Technol [Internet]. 3 September 2024 [dikutip 19 November 2025];6(2):236–48. Tersedia pada: https://www.ajol.info/index.php/cajost/article/view/277683
10. Abou Hussein EM, Shaban SE, Makhlouf SA. Unveiling the effect of CeO2 addition on optical, physical and radiation shielding efficiency in binary lead borate glasses. Radiat Phys Chem [Internet]. Oktober 2025 [dikutip 18 November 2025]; 235:112762. Tersedia pada: https://linkinghub.elsevier.com/retrieve/pii/S0969806X25002543
11. Solak BB, Aktas B, Yilmaz D, Kalecik S, Yalcin S, Acikgoz A, dkk. Exploring the radiation shielding properties of B2O3-PbO-TeO2-CeO2-WO3 glasses: A comprehensive study on structural, mechanical, gamma, and neutron attenuation characteristics. Mater Chem Phys [Internet]. Januari 2024 [dikutip 19 November 2025]; 312:128672. Tersedia pada: https://linkinghub.elsevier.com/retrieve/pii/S0254058423013809
12. Sayyed MI, More CV, Hanfi MY, Kamath SD. Impact of BaO on the gamma-ray shielding performance of lanthanum barium-borate glasses. Sci Rep [Internet]. 23 Oktober 2025 [dikutip 19 November 2025];15(1):37009. Tersedia pada: https://www.nature.com/articles/s41598-025-13248-0
13. Berger MJ, Hubbell JH, Seltzer SM, Chang J, Coursey JS, Sukumar R, dkk. XCOM: Photon Cross Sections Database. 2010;
14. Al-Buriahi MS, Echeweozo EO, Sriwunkum C, Alomayrah N, Alzahrani JS. Gamma Radiation Shielding and Interaction Properties of MoO3-Doped Cadmium Zinc Lithium-Borate Glasses. Nucl Eng Technol [Internet]. November 2024 [dikutip 19 November 2024];S1738573324005631. Tersedia pada: https://linkinghub.elsevier.com/retrieve/pii/S1738573324005631
15. Hoşgör G, Tabar E, Kemah E, Yakut H. Influence of TiO2 content on the radiation shielding properties of the La2O3-B2O3-Gd2O3-Nb2O5-ZrO2-SiO2 glasses. Radiat Phys Chem [Internet]. Januari 2025 [dikutip 18 Oktober 2024]; 226:112281. Tersedia pada: https://linkinghub.elsevier.com/retrieve/pii/S0969806X24007734
16. Es-soufi H, Ouaha A, Sayyed MI, Bih H, Bih L. Impact of Nb2O5 on radiation shielding properties of the bismuth-titanium-phosphate glasses. Optik [Internet]. Maret 2023 [dikutip 27 Agustus 2025]; 274:170511. Tersedia pada: https://linkinghub.elsevier.com/retrieve/pii/S0030402623000074
17. Abdalsalam AH, Şakar E, Kaky KM, Mhareb MHA, Ceviz Şakar B, Sayyed MI, dkk. Investigation of gamma ray attenuation features of bismuth oxide nano powder reinforced high-density polyethylene matrix composites. Radiat Phys Chem [Internet]. Maret 2020 [dikutip 22 September 2024]; 168:108537. Tersedia pada: https://linkinghub.elsevier.com/retrieve/pii/S0969806X19302531
18. Al-Buriahi MS, Kurtulus R, Eke C, Alomairy S, Olarinoye IO. An insight into advanced glass systems for radiation shielding applications: A review on different modifiers and heavy metal oxides-based glasses. Heliyon [Internet]. November 2024 [dikutip 19 November 2024];10(22):e40249. Tersedia pada: https://linkinghub.elsevier.com/retrieve/pii/S2405844024162809

19. Alomari AH. Assessing the contribution of MoO3 and WO3 additions on sodium phosphate glasses: Elastic moduli and radiation shielding properties. J Radiat Res Appl Sci [Internet]. September 2025 [dikutip 18 November 2025];18(3):101786. Tersedia pada: https://linkinghub.elsevier.com/retrieve/pii/S1687850725004984
20. Nasrabadi M, Tavakoli-Anbaran H, Ebrahimibasabi E. Experimental study of radiation shielding and mechanical properties of polymer nanocomposite reinforced with CeO2 NPs. Mater Today Commun [Internet]. September 2025 [dikutip 5 November 2025]; 48:113369. Tersedia pada: https://linkinghub.elsevier.com/retrieve/pii/S2352492825018811

How to cite this article: Oki Ade Putra, Zaenul Muhlisin, Much. Azam, Pandji Triadyaksa. Computational evaluation of CeO_2-Modified tungsten borate glasses as lead-free gamma-ray shielding materials. *International Journal of Research and Review*. 2026; 13(6): 158-167. DOI: *https://doi.org/10.52403/ijrr.20260616*

******